On the morphology and corrosion behavior of Ni nanostructures electrodeposited in the presence of different surfactants

Mahdieh Zolfaghari, Ali Arab*, Alireza Asghari
Department of Chemistry, Semnan University, Semnan, Iran.

Abstract

In this work, Ni nano structures with different surface morphology have been electrodeposited from the Waths bath using different techniques in the presence of three types of surfactants. CTAB, SDS, and Triton x-100 have been used as cathionic, anionic and nonionic surfactants respectively. The surfactants concentration have been selected at below, equal to and above the corresponding critical micelle concentration (CMC). The SEM analyses show that the porosity and homogeneity of the electrodeposited samples depend on the surfactant type and its concentration. In the presence of CTAB, electrodeposition process has been certainly hindered in some region. For SDS, nano-particles with the same charges repel each other and disperse in a more uniform way. In the presence of Triton x-100, agglomeration of particles is seen and particles are not dispersed. The corrosion behavior of electrodeposited samples has also been investigated in 1 M NaOH solution using Tafel potentiodynamic polarization method as well as electrochemical impedance spectroscopy analyses. It is observed that all samples have low corrosion current density and the sample prepared above the CMC point of SDS has the lowest corrosion rate. In addition, according to our findings, the electrodeposited samples using DC method have larger particle sizes and lower corrosion rate.

1. Introduction

Recent developments in electrodeposition technology have led to the fabrication of nanostructured coatings with a multilayered structure that increasingly makes their rout into the industrial use and meet the demands of more severe applications [1]. Electrodeposition technique offers several advantages such as room temperature operation, low energy requirements, the capability to coat complex component geometries, low cost and simple scale-up for larger components [2]. In recent years, the tendency to produce nano structures from electroplating baths has increased due to their superior properties. Electrodeposition of nanocrystalline nickel and its alloys has been the subject

*.**Corresponding author:** Assistant Professor of Physical Chemistry, Semnan University, Faculty of Chemistry. Email address: a.arab@semnan.ac.ir

of many studies because of technological importance [3–8].

Most of these studies have been focused on the mechanism and properties of Ni electrodeposits obtained from sulfate or sulfate–chloride electrolytes with a special emphasis on using Watts bath. Nasirpour et al. have reported that electrodeposition conditions affect microstructure, cathodic efficiency, micro hardness, magnetic and corrosion properties of nickel films. They used three methods including Pulse Current (PC), Pulse Reverse Current (PRC), and Direct Current (DC) for nickel electrodeposition. Borkar and Harimkar have reported that electrodeposition of nickel with PC and PRC methods reduces the grain size and surface roughness of films compared to the DC method [9].

Uniform dispersion of particles in electrolytes can increase their participation in the coating and improve the coating properties. To date, various physical and chemical methods have been used for this purpose. Physical techniques, such as using destructive energies (e.g. ultrasonic waves) can break down the nano-particles bonding and inhibit the agglomeration [10]. In the chemical techniques, surfactants are used and absorbed on the surface of nano-particles. In this way, the repulsion force between particles with the same charges will increase. This, in turn, reduces the agglomeration and provides a solution with more stable particles. Many surfactants assemble in the bulk solution into aggregates known as micelles. As the interface becomes saturated, the molecules start to form aggregates or micelles in the bulk. The concentration that surfactants begin to form micelles is known as the critical micelle concentration (CMC). Many researchers have studied the effects of different surfactants in the plating baths [11-17].

In the present study, we attempt to examine the effect of three types of surfactants on the morphology of Ni nano structures. CTAB, SDS, and triton x-100 were used as cationic, anionic and nonionic surfactants respectively. Nanocrystalline nickel films were electrodeposited by DC and PRC techniques on a copper substrate to exploit the effect of electrodeposition conditions as well as

surfactant's type on the structure and morphology of electrodeposited films. Also, the corrosion behavior of electrodeposited samples was investigated in the alkaline solution using potentiodynamic polarization method.

2. Experimental

2.1. Materials

Nickel sulfate ($NiSO_4.6H_2O$), Nickel chloride ($NiCl_2.6H_2O$), Boric acid (H_3BO_3), Sodium hydroxide (NaOH), Nitric acid (HNO_3), cathionic surfactant (CTAB), anionic surfactant (SDS), and nonionic surfactant (triton x-100) were purchased from Merck company. All the chemicals were of analytical grade and were used as received. All solutions were prepared with double distilled water. Copper foils (99.9% purity) were used as the substrate for the electrodeposition of Ni nanostructures.

2.2. Preparation and methods

In this study, different Ni nano structures were electrodeposited from a Watts bath in the presence of different surfactants at pH of 3.16. During electrodeposition process, the electrolyte was stirred using a magnetic stirrer at a rate of ٤٠٠ rpm. Electrodeposition of samples was done in a standard three-electrode cell. A platinum electrode and a set of Ag/AgCl electrode were used as the counter and reference electrodes, respectively. The copper foils with the surface area of 1 cm^2 were used as working electrodes. Before electrodeposition, the electrode surface was polished by the emery papers with the grift sizes of 2000, 2500, and 3000, then washed with distilled water, dipped into a dilute HNO_3 solution for 1 min followed by a rinse with distilled water and then immediately immersed in the bath solution. The chemical composition of electrodeposition bath is shown in Table 1. The concentration of surfactants is chosen in the forms of below, equal to and above the corresponding CMC points. Electrodeposition process was carried out through DC and PRC methods. In DC method, the current density of -100 mA cm^{-2} was continuously exerted to the electrode for 150 s. In PRC

method, the current density was changed between -100 mA cm^{-2} and 100 mA cm^{-2} according to the Fig. 1 for 150 s. Nine Ni samples were prepared according to the preparation conditions shown in Table 2. The corrosion behavior of electrodeposited samples was investigated in 1 M NaOH solution using Tafel potentiodynamic polarization method. All electrochemical experiments were carried out at room temperature by an Ivium Stat Potentiostat/Galvanostat run by a PC through its commercial software's. The electrochemical impedance experiments were performed using an Origaflex Potentiostat/Galvanostat model OGF500. The frequency range of 100 kHz to 50 mHz and AC amplitude of 10 mV were selected for all impedance measurements. Surface morphology of the samples was examined by scanning electron microscopy (SEM) on a FE-SEM microscope model HITACHIS-4160.

Table 1. The chemical composition of Watts bath for the electrodeposition of samples.

Concentration	Compound
330 g/l	NiSO$_4$.6H$_2$O
45g/l	NiCl$_2$.6H$_2$O
37g/l	H$_3$BO$_3$
50[1], 350[2], 450[3] mg/l	CTAB
500[1], 2300[2], 3000[3] mg/l	SDS
1.35[1], 1.90[2], 3.29[3] mg/l	Triton x-100

[1]below CMC concentration, [2]equal to CMC concentration, and [3]*above* CMC concentration.

Table 2. Preparation conditions of different samples.

Sample name	Method	Surfactant
Ni-CTAB[1]		
Ni-CTAB[2]	PRC	CTAB
Ni-CTAB[3]		
Ni-SDS[1]		
Ni-SDS[2]	PRC	SDS
Ni-SDS[3]		
Ni-Triton[1]		
Ni-Triton[2]	DC	Triton x-100
Ni-Triton[3]		

[1]below CMC concentration, [2]equal to CMC concentration, and [3]above CMC concentration.
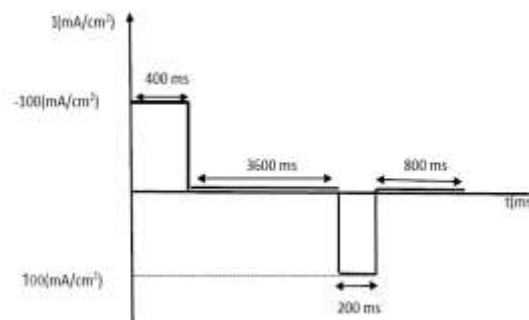
**Fig. 1.** Schematic presentation of PRC method.

3. Results and discussion
3.1. FE-SEM results

The SEM images of electrodeposited samples are presented in Figs.2-4. As shown in these figures, the surface morphology and structure of the samples is strongly depended on the concentration of surfactants in the Watts bath as well as surfactant type.

Fig. 2(a-c) presents the FE-SEM images of electrodeposited Ni samples in the presence of CTAB, SDS, and Triton x-100 respectively where the concentration of all surfactants in the electrodeposition bath is below the corresponding CMC point. When using CTAB as a cationic surfactant, the repulsion between free monomers of surfactant and dissolved cations (Ni^{2+}) makes the motion of the cations toward the electrode surface faster and causes a high degree of nucleation. So the process results in a high homogeny and a high number of the particles on a certain area of the electrode.

In the presence of SDS as an anionic surfactant (Fig. 2b), free monomers of surfactant surround the cations. Therefore, the motion of Ni^{2+} cations toward the electrode surface is slow and the nucleation process proceeds slowly. The remaining cations are deposited gradually on the created nucleus and make large-sized particles.

Fig. 2c indicates that in the presence of triton as a non-ionic surfactant a uniform nucleation with small average particle sizes has occurred on the surface of the substrate. In fact, due to the neutrality nature of the surfactant, the Ni^{2+} cations suffer randomly non oriented dispersion forces induced from the surfactant and so the deposition proceeds in a more uniform way.
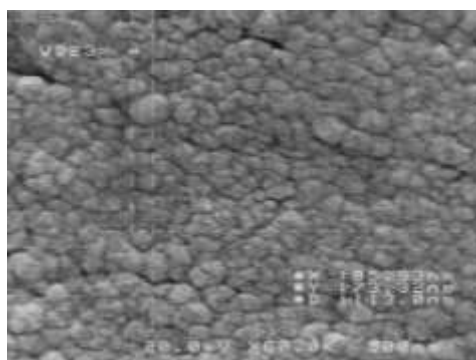
(a) Ni-CTAB[1]
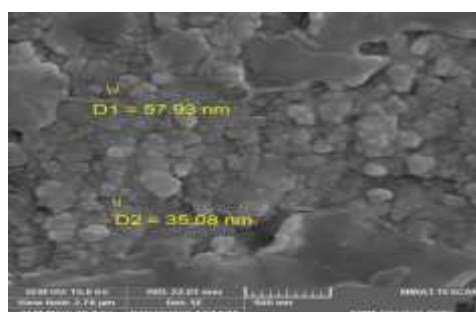
(b) Ni-SDS[1]
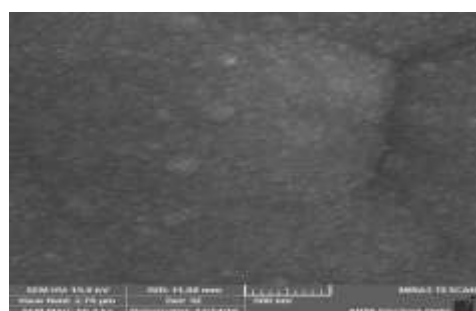
(c) Ni-Triton[1]

Fig. 2. The FE-SEM images of electrodeposited Ni samples in the presence of CTAB (a), SDS (b), and Triton x-100 (c). The concentration of all surfactants in the bath is below the corresponding CMC points.

Fig. 3(a-c) shows the FE-SEM images of the electrodeposited Ni samples from solutions containing CTAB, SDS, and Triton x-100 surfactants respectively. The concentration of surfactants is equal to the corresponding CMC point where the micelle formation is started.

Compared to the Fig. 2a by increasing the concentration of CTAB to the CMC value the particle sizes are increased considerably (Fig. 3a). This can be due to the higher dispersion degree of the cations which reduces the nucleation and the gradual growth of the nucleus

creates increased particles sizes on a certain area of the electrode. The formed micelles with the positive charges cause higher dispersion of Ni^{2+} cations.

By increasing the concentration of SDS to the CMC value, the concentration of free monomers reduces because of the formation of micelles. The formed micelles are also negatively charged which attract Ni^{2+} cations. Ni^{2+} cations adsorbed on the surface of the micelles move to the electrode surface and after electron transfer to the Ni^{2+} cations, the micelles come back to the solution. Therefore, a uniform and smaller particle sizes (Fig. 3b) compared to the Fig. 2b is obtained.
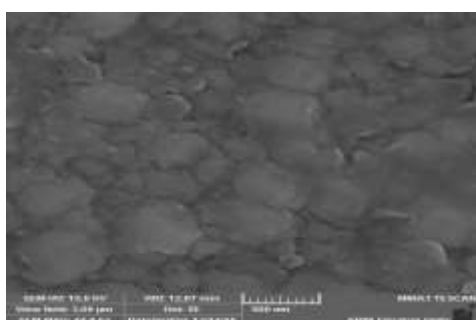
When using triton as a non-ionic surfactant at CMC point, the neutral micelles retard the motion of the Ni^{2+} cations toward the electrode surface and a low nucleation has occurred. So, large average particle sizes are resulted due to the gradual growth of the formed nucleus.

Fig. 4a-c shows the FE-SEM images of the electrodeposited samples in the presence of CTAB, SDS, and Triton x-100, respectively. The concentration of all surfactants was selected above the corresponding CMC points. Above the CMC point, the free monomers of surfactants, as well as micelles, are both presents in the solution.
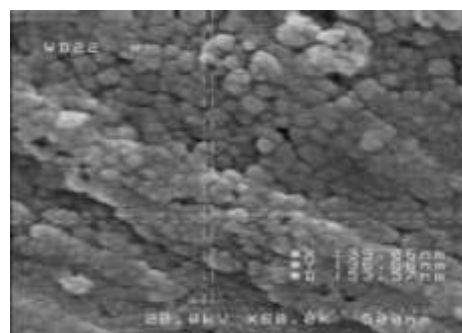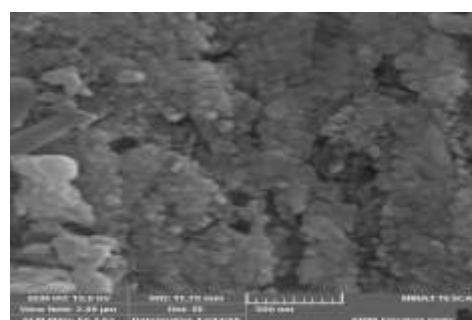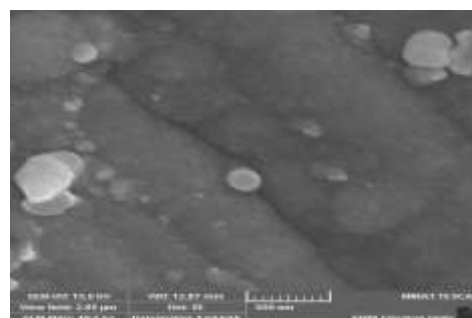
The repulsion between CTAB surfactant and cations above the CMC point is increased and creates a high degree nucleation (Fig. 4a). The particle sizes are therefore smaller compared to the Fig. 2a.

With increasing the concentration of anionic SDS surfactant above the CMC point a high degree of nucleation is observed (Fig. 4b). The surrounded cations

with the free monomers or micelles create small sized particles. When the triton concentration is above the CMC (Fig. 4c), the dispersion rate of the cations is increased considerably. So the motion of the cations towards the substrate and nucleation process is decreased. The result of the decreased nucleation rate is very large particles. The FE-SEM images of Ni-CTAB[1], Ni-CTAB[2], and Ni-CTAB[3] samples (Figs. 2a, 3a, and 4a) indicate that the effect of cationic surfactant (CTAB) on the surface morphology is significant.
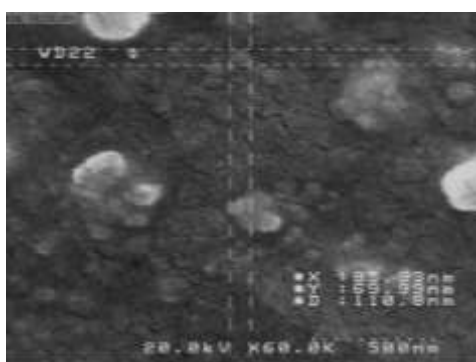
(a) Ni-CTAB[3]
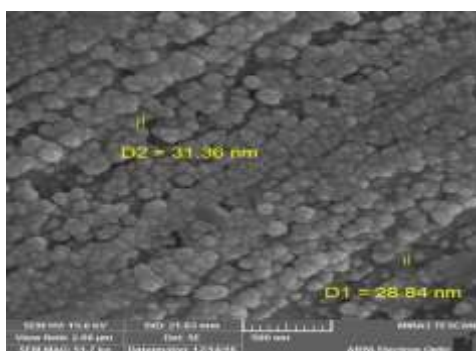
(a) Ni-CTAB[2]

(b) Ni-SDS[3]

(b) Ni-SDS[2]

(c) Ni-Triton[3]

Fig. 4. The FE-SEM images of electrodeposited Ni samples in the presence of CTAB (a), SDS (b), and Triton x-100 (c). The concentration of all surfactants in the bath is above the corresponding CMC points.

(c) Ni-Triton[2]

Fig. 3. The FE-SEM images of electrodeposited Ni samples in the presence of CTAB (a), SDS (b), and Triton x-100 (c). The concentration of all surfactants in the bath is equal to the corresponding CMC points.

It seems that electrodeposition process has been certainly hindered in some regions because of probable adsorption of CTAB on the electrode surface in the forward current.

SDS (an anionic surfactant) could be absorbed on the surface of nanoparticles. In this way, nano-particles with the same charges repel each other and disperse in a more uniform way (Figs. 2b, 3b, and 4b).

In Ni-Triton[1], Ni-Triton[2], and Ni-Triton[3] samples (Figs. 2c, 3c, and 4c) we guess particles stick together. A large accumulation of particles was seen in some areas of the electrode surface that creates a big hunks and reduces the surface area. In addition, agglomeration of particles was seen in this type of surfactant and particles were not dispersed.

3.2. The corrosion study of samples

The corrosion behavior of electrodeposited samples was investigated in 1 M NaOH solution using Tafel potentiodynamic polarization method. In all experiments, the samples were immersed in 1 M NaOH solution for 15 minutes in order to obtain a constant open circuit potential. The Tafel plots were recorded in the range of ±300 mV around the open circuit potential in the anodic direction with the scan rate of 2 mV s^{-1}. Figs. 5-7 present the Tafel plots of samples electrodeposited below, equal to, and above the CMC point respectively. The corresponding corrosion parameters including corrosion current densities (i_{corr}), corrosion potential (E_{corr}), cathodic Tafel slope (b_c), and anodic Tafel slope (b_a) are also reported in Tables 3-5.

According to the Fig . 5 and Table 3, below the CMC point the Ni-sample that deposited in the presence of SDS surfactant has the most positive corrosion potential (-0.27 V) and the lowest corrosion current density (2.89×10^{-6} A/cm^2). As mentioned earlier, when we used SDS at below the CMC point Ni^{2+} particles had the highest level of participation in metal coatings. It seems that the incorporation of Ni^{2+} particles in the coating plays a major role in improving the corrosion resistance of the coatings. They could fill all pores and micro-holes of the coatings and decreased the tendency of the coatings to corrosion.

Table 3. The corrosion parameters of Ni samples electrodeposited at surfactant concentration below the CMC point according to the Tafel plots of Fig 5.

Sample	Ni-CTAB[1]	Ni-SDS[1]	Ni-Triton[1]
E_{corr} (V)	-0.49	-0.27	-0.55
i_{corr} (A/cm^2)	3.20×10^{-6}	2.89×10^{-6}	3.65×10^{-6}
b_a (V/dec)	0.033	0.037	0.063
b_c (V/dec)	0.041	0.028	0.041
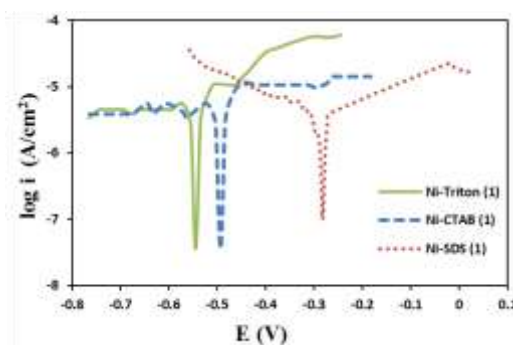
Fig. 5. The Tafel plots recorded in 1 M NaOH solution for Ni samples electrodeposited at surfactant concentration below the CMC point.

At concentration equal to the CMC point, according to the Fig. 6 and Table 4, it is clear that the sample electrodeposited in the presence of Triton has the lowest corrosion current density (2.4×10^{-6} A/cm^2). When Triton in CMC concentration used, large average particle sizes are resulted due to the gradual growth of the formed nucleus and it seems they could fill all pores and micro-holes of the coatings and decrease the corrosion tendency of the coatings.

The electrochemical impedance measurements were also performed at concentration equal to the CMC point at corrosion potentials reported in Table 4. The obtained Nyquist diagrams are presented in Fig. 7 and the corresponding equivalent circuit compatible with the experimental Nyquist diagrams is also presented as the inset of Fig. 7. The Nyquist diagrams consist of a distorted semicircle and its diameter presents the charge transfer resistance related to the corrosion reaction (R_{ct}). In this figure, R_s demonstrates ohmic resistance of the electrolyte, Constant phase element (*CPE*) which is given by eq. 1[18] represents the character of the double layer.

$$Z_{CPE}(\omega) = [T(j\omega)^n]^{-1} \qquad (1)$$

Where ω is the angular frequency of the AC signal, j is equal to $\sqrt{-1}$, n is related to the roughness of the electrode with the values in the 0 to 1 range. T is related to the double layer capacitance according to the $C_{dl} = T^{1/n}R_{ct}^{(1-n)/n}$ relationship [18].

The calculated values of R_s, R_{ct}, n, and T are reported in Table 5. It is clear that for Ni-Triton[2] sample the value of R_{ct} is significantly greater compared to the Ni-

CTAB[2] and Ni-SDS[2] samples indicating lower corrosion rate of this sample in accord with the Tafel potentiodynamic polarization results.
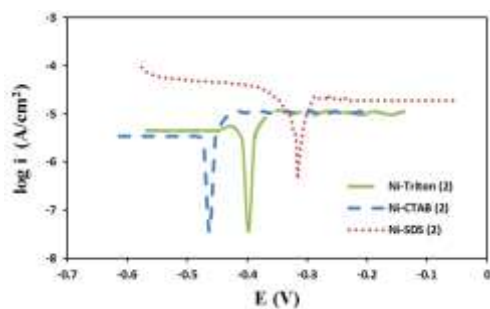
Fig. 6. The Tafel plots recorded in 1 M NaOH solution for Ni samples electrodeposited at surfactant concentration equal to the CMC point.

Table 4. The corrosion parameters of Ni samples electrodeposited at surfactant concentration equal to the CMC point according to the Tafel plots of Fig 6.

Sample	Ni-CTAB[2]	Ni-SDS[2]	Ni-Triton[2]
E_{corr} (V)	-0.51	-0.29	-0.40
i_{corr} (A/cm^2)	3.30×10^{-6}	2.90×10^{-5}	2.40×10^{-6}
b_a (V/dec)	0.212	0.044	0.063
b_c (V/dec)	0.078	0.873	0.042

According to the Fig 8 and Table 6, It is clear that above the CMC point the sample deposited with SDS has the most positive corrosion potential (-0.28 V) and the lowest corrosion current density (2.30×10^{-6} A/cm^2).

The results of tables 4 and 6 show that the values of the Tafel slopes for some of the samples are higher than the expected values. It should be noticed that the Tafel slopes are indeed potential dependent and, in turn, coverage dependent. In the literature, various Tafel slopes have been reported. The high values of Tafel slopes are related to the formation of oxide films on the surface of electrodes.

Table 5. Calculated equivalent circuit parameters for the corrosion of Ni samples electrodeposited at surfactant concentration equal to the CMC point.

sample	R_s/Ω cm^2	R_{ct}/Ω cm^2	n	T/Ω^{-1} cm^{-2} s^n
Ni-SDS[2]	1.24	943.1	0.70	0.0000222
Ni-CTAB[2]	2.01	2858	0.80	0.0000276
Ni-Triton[2]	1.14	16686	0.89	0.0000699
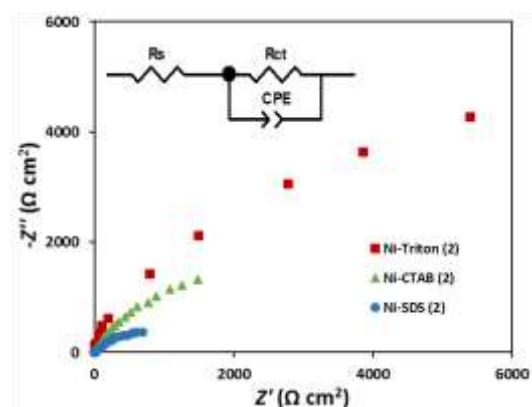
Fig. 7. The Nyquist diagrams recorded in 1 M NaOH solution for Ni samples electrodeposited at surfactant concentration equal to the CMC point, inset: The equivalent circuit compatible with the experimental Nyquist diagrams.
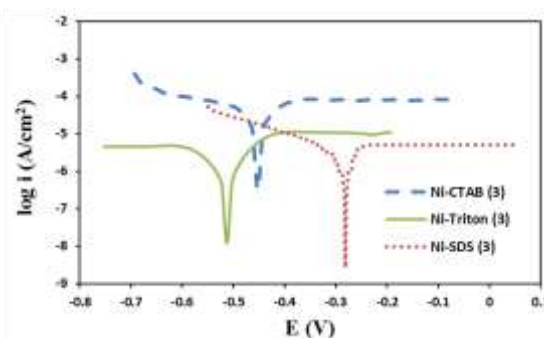
Fig. 8. The Tafel plots recorded in 1 M NaOH solution for Ni samples electrodeposited at surfactant concentration above the CMC point.

Table 6. The corrosion parameters of Ni samples electrodeposited at surfactant concentration above the CMC point according to the Tafel plots of Fig 8.

Sample	Ni-CTAB[3]	Ni-SDS[3]	Ni-Triton[3]
E_{corr} (V)	-0.45	-0.28	-0.53
i_{corr} (A/cm^2)	1.17×10^{-5}	2.30×10^{-6}	2.60×10^{-6}
b_a (V/dec)	0.381	0.039	0.219
b_c (V/dec)	0.426	0.207	0.219

4. Conclusion

Nanostructured Ni samples were electrodeposited from Watts bath containing different surfactants including CTAB, SDS and Triton x100 using DC and PRC techniques. It was observed that surfactant type, as well as surfactant concentration, affected the porosity and homogeneity of the electrodeposited samples. The effect of cationic surfactant (CTAB) on the surface morphology was significant and electrodeposition process was certainly hindered in some regions because of probable adsorption of CTAB on the electrode surface. SDS (an anionic surfactant) could be absorbed on the surface of nanoparticles. In this way, nano-particles with the same charges repel each other

and disperse in a more uniform way. For nonionic surfactant (Triton x-100), A large accumulation of particles was seen in some areas of the electrode surface that creates a big hunks and reduces the surface area. In addition, agglomeration of particles was seen in this type of surfactant and particles were not dispersed.

The corrosion of electrodeposited samples was investigated in 1 M NaOH solution employing Tafel potentiodynamic polarization method and electrochemical impedance spectroscopy analyses. It was observed that the incorporation of nano particles of Ni in the coating played a major role in improving the corrosion resistance of the coatings. According to our findings, the sample prepared above the CMC point of SDS had the highest resistance against corrosion. When we used SDS, the particles could fill all pores and micro-holes of the coatings and decreased the tendency of the coatings to corrosion. Finally, according to our results, the electrodeposited samples using DC method had larger particle sizes and lower corrosion rate.

References

[1] R.K. Saha, T.I. Khan, Surf. Coat. Technol., **205** (2010) 890.

[2] M. Sabri, A.A. Sarabi, S.M. Naseri Kondelo, Mater. Chem. Phys., **136** (2012) 566.

[3] A. Cziraki, B. Fogaassy, I. Geroces, E. Toth-Kadar, I. Bakonyi, J. Mater. Sci., **29** (1994) 4771.

[4] A. Cziraki, Z. Tonkovics, I. Geroces, B. Fogarassy, I. Groma, E. Toth-Kadar, T. Tarnoczi, I. Bakonyi, Mater. Sci. Eng. A, **179-180** (1994) 531.

[5] I. Bakonyi, E. Toth-Kadar, T. Tarnoczi, L.K. Varga, A. Cziraki, I. Geroces, B. Fogarassy, Nanostruct. Mater. **3** (1993) 155.

[6] S .Lauer, Z. Guan, H .Wolf, H. Natter, M .Schmelzer, R. Hempelmann, Nanostruct. Mater. **12** (1999) 955.

[7] M.J. Aus, B .Szpunar, A.M. El-Sherik, U. Erb, G. Palumbo, K.T. Aust , Scr. Metall. Mater., **27** (1992) 1639.

[8] H. Wolf, Z. Guan, X. Li, T. Wichert, Hyperfine Interact.**136** (2001) 281.

[9] F. Nasirpouri, M.R. Sanaeian, A.S. Samardak, E.V. Sukovatitsina, A.V. Ognev, L.A. Chebotkevich, M.G. Hosseini, M. Abdolmaleki, Appl. Surf. Sci, **292** (2014) 795.

[10] S.L. Kuo, Y.C. Chen, M.D. Ger, W.H. Hwu, Mater. Chem. Phys., **86** (2004) 5.

[11] M. Ger, Mater. Chem. Phys., **87** (2004) 67.

[12] L. Chen, L. Wang, Z. Zeng, J. Zhang, Mater. Sci. Eng. A, **434** (2006) 319-325.

[13] M. Wang, J. Appl. Electrochem., **38** (2008) 245.

[14] A.A. Amadeh, Int. J. Mod. Phys. B, **22** (2008) 3037.

[15] C. Guo, Y. Zuo, X. Zhao, J. Zhao, J. Xiong, Surf. Coat. Technol., **202** (2008) 3385.

[16] E. Pompei, L. Magagnin, N. Lecis, P.L. Cavallotti, Electrochim. Acta, **54** (2009) 2571.

[17] H. Gul, F. Kilic, S. Aslan, A. Alp, H. Akbulut, Wear, **267** (2009) 976.

[18] M.G. Hosseini, E. Ariankhah, Journal of Applied Chemistry, **11** (2017) 147.